Acta Crystallographica Section B
Structural Science, Crystal Engineering and Materials
ISSN 2052-5192

Crystal and magnetic structures of hexagonal $YMnO_3$

Christopher J. Howard,[a]* Branton J. Campbell,[b] Harold T. Stokes,[b] Michael A. Carpenter[c] and Richard I. Thomson[c]

[a]School of Engineering, University of Newcastle, Callaghan, NSW 2308, Australia, [b]Department of Physics and Astronomy, Brigham Young University, Box 4675, Provo, Utah 84602, USA, and [c]Department of Earth Sciences, University of Cambridge, Downing Street, Cambridge CB2 3EQ, England

Correspondence e-mail: chris.howard@newcastle.edu.au

Received 23 February 2013
Accepted 1 November 2013

The available data on the structural and magnetic transitions in multiferroic hexagonal $YMnO_3$ have been reviewed, first making use of the computer programs from the group theoretical *ISOTROPY* software suite to list possible crystal and magnetic structures, then taking into account the capability of neutron diffraction and other physical methods to distinguish them. This leads to a clear view of the transformation sequence, as follows. Hexagonal $YMnO_3$ is paraelectric in $P6_3/mmc$ at elevated temperatures, and undergoes a single structural transition on cooling through 1250 K to a ferrielectric phase in $P6_3cm$ that is retained through room temperature. At a much lower temperature, 70 K, there is a magnetic transition from paramagnetic to a triangular antiferromagnetic arrangement, most likely with symmetry $P6_3'cm'$. Comment is made on the unusual coupling of ferroelectric and magnetic domains reported to occur in this material, as well as on the so-called 'giant magneto-elastic' effect.

1. Introduction

The hexagonal manganite $YMnO_3$ has attracted a great deal of interest, especially in recent times, because it is a practical ferroelectric at room temperature that, at low temperature, also shows magnetic ordering (Yakel *et al.*, 1963; Bertaut, Fang & Forrat, 1963; Benedek *et al.*, 2012; Bertaut & Mercier, 1963; Bertaut *et al.*, 1965; Fiebig *et al.*, 2000). The manganite shows, in addition, evidence for coupling between the polarization and the magnetic ordering. A dielectric anomaly has been observed at the Néel point (Huang *et al.*, 1997; Katsufuji *et al.*, 2001), and it has been reported from observations of second harmonic generation (SHG) that there is a reversal of the (antiferro-) magnetic order parameter at ferroelectric domain boundaries (Fiebig *et al.*, 2002). The physics of this apparent magneto-electric coupling is of particular interest within the context of magneto-electric and multiferroic materials and their potential applications (Fiebig, 2005; Eerenstein *et al.*, 2006). More recently, a 'giant magneto-elastic coupling' has been claimed to occur (Lee *et al.*, 2008).

The purpose of this communication is to critically review the available data on the crystal and magnetic structures, the phase transitions, and the diverse couplings in $YMnO_3$. As in previous work (Howard & Stokes, 2005; Howard & Carpenter, 2012), we make use of group theoretical analysis as implemented in the *ISOTROPY* suite of computer programs, including *ISOTROPY* (Stokes *et al.*, 2007) and *ISODISTORT* (Campbell *et al.*, 2006). The work reported here is used elsewhere (Thomson *et al.*, 2014) to assist the interpretation of recent studies by resonant ultrasound spectroscopy (RUS) of

the elastic anomalies associated with the phase transitions observed.

2. Crystal structures and the structural transition(s)

It was recognized at the outset (Yakel *et al.*, 1963) that $YMnO_3$ would be ferroelectric at room temperature, and indeed it shows a spontaneous polarization that has been recorded as $\sim 5\ \mu C\ cm^{-2}$ (Smolenski & Bokov, 1964). The microscopic origin of the polarization has been explained by a number of authors (Benedek *et al.*, 2012; Van Aken *et al.*, 2004; Gibbs *et al.*, 2011) on the basis of its crystal structure. It is best understood by comparing the room-temperature structure, in space group $P6_3cm$, with that of the high-temperature paraelectric structure in space group $P6_3/mmc$. The paraelectric structure can be described as layers of corner-linked MnO_6 trigonal bipyramids, separated by layers of Y. In the ferroelectric (or more strictly ferrielectric) structure there is tilting of the MnO_6 trigonal bipyramids, along with buckling in the layers of Y (see Fig. 1). On the basis of recent room-temperature structure determinations (Gibbs *et al.*, 2011; van Aken *et al.*, 2001), it is found that the Mn^{3+} stays close to the centre of the MnO_6 bipyramid, and 90% or more of the net polarization arises from the movements of Y^{3+} ions (relative to the MnO_6 layers) parallel and antiparallel to the hexagonal axis, the numbers moving in the opposite senses being in the ratio two to one. Calculations of polarization based on these structural data (Gibbs *et al.*, 2011) give results close to the measured values.

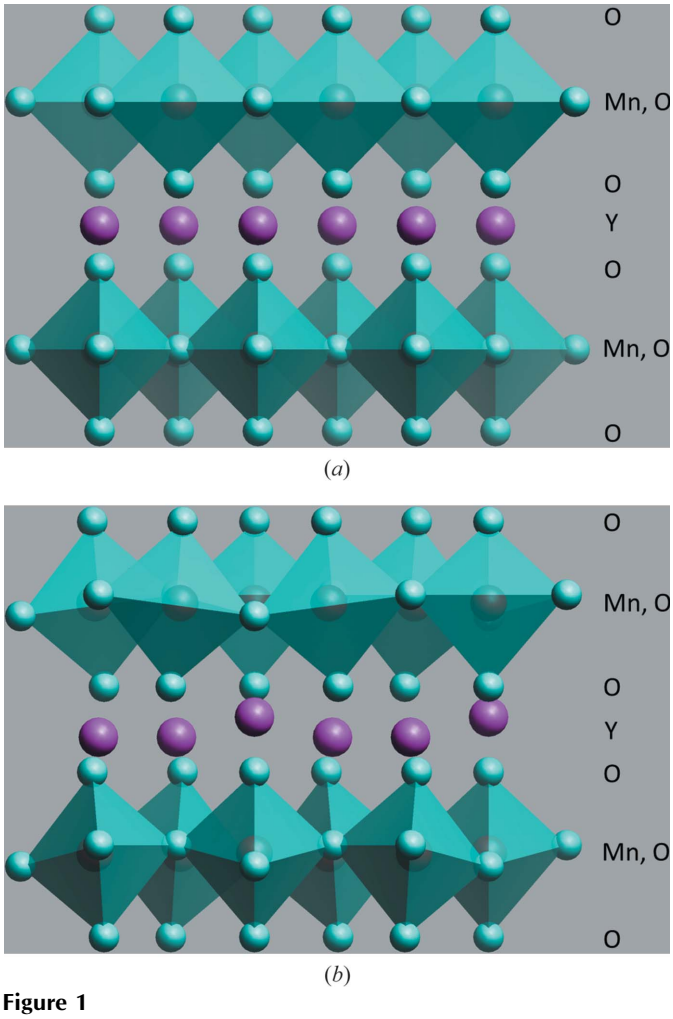

Figure 1
(*a*) The high-temperature and (*b*) room-temperature crystal structures of $YMnO_3$, drawn from the data of Gibbs *et al.* (2011) using the *ATOMS* (Dowty, 1999) computer program. The polarization at room temperature is mostly due to displacement of Y^{3+} ions relative to the rest of the structure – one Y^{3+} moves upwards and two move down.

There have been claims in the literature (Van Aken *et al.*, 2004; Lonkai *et al.*, 2004) that the transition from the paraelectric structure in $P6_3/mmc$ to the ferroelectric structure in $P6_3cm$ must proceed *via* an intermediate phase, along with some claim of supporting experimental evidence. The possible intermediates are a structure with tilting of the MnO_6 bipyramids but without buckling, in space group $P6_3/mcm$, or the uniform displacement of atoms, say the Y atoms, parallel to the hexagonal axis, in space group $P6_3mc$.[1] A single distortion, combining tilting of the MnO_6 bipyramids and shifts parallel to the hexagonal axis (no longer uniform, hence buckling) to achieve the low-temperature structure, would seem a more plausible scenario. The group-theoretical analysis (Lonkai *et al.*, 2004; Fennie & Rabe, 2005; Gibbs *et al.*, 2011; Thomson *et al.*, 2014), using *ISOTROPY* (Stokes *et al.*, 2007), shows three possible scenarios:

(1) an initial reduction in symmetry to $P6_3/mcm$ mediated by irrep K_1 (using notation of Miller & Love, 1967) of the $P6_3/mmc$ parent, followed by a second transition to $P6_3cm$;

(2) a reduction in symmetry to $P6_3mc$ mediated by irrep Γ_2^-, followed by a second transition;

(3) a single transition $P6_3/mmc$ to $P6_3cm$ with K_3 as the active irrep.

According to *ISOTROPY*, and in agreement with the description given above, the single transition *via* irrep K_3 can be continuous, whereas for each of the two-step scenarios at least one of the transitions is discontinuous. Consistent with this, Fennie & Rabe (2005) find from their group-theoretical analysis and first-principles density functional calculations that there is a single zone-boundary instability (K_3) that couples strongly to the polarization. The claim that there must be an intermediate (Lonkai *et al.*, 2004; Van Aken *et al.*, 2004) seems to be based largely on the premise that a zone boundary instability cannot lead to polarization; however, this overlooks the fact that a K_3 driving instability would be accompanied by the Γ_2^- zone-centre distortion as a secondary, and that does lead to spontaneous polarization. The fact that K_3 implies a secondary Γ_2^- distortion seems also to have been overlooked in other arguments for the two transition scenario (Kim *et al.*, 2010). From an experimental point of view, it is significant that, in their high-resolution neutron powder diffraction study, Gibbs *et al.* (2011) determined the space-group symmetry to be $P6_3cm$ (as per the room-temperature structure) at 1243 K, just below the transition to the paraelectric phase, and significant too that their lattice parameter data show no

[1] In this structure, with the same unit cell as the $P6_3/mmc$ parent, there is only one Y atom per layer per unit cell, so all these Y must move in unison.

evidence for any phase transition between this and room temperature. We are not persuaded that at around 920 K there is an isosymmetric transition (necessarily first order according to *ISOTROPY*, see also Christy, 1995), nor of the increase in polarization (mode Γ_2^-) they report above this temperature. Finally, our own RUS data (Thomson *et al.*, 2014) contain no hint of any second structural transition (isosymmetric or otherwise) between the high-temperature transition, at around 1250 K, and room temperature.

Abrahams (2009) has carried out a coordinate analysis of the different structures proposed for $YMnO_3$, and has postulated that at higher temperatures there may be a higher symmetry aristotype, in the space group *P*6/*mmm*. This is the structure that would be formed if the apical O (see Fig. 1*a*) were to move into the plane occupied by Y. This would lead to considerably shorter Y—O distances unless compensated by relatively large increases in the *a* parameter, and the structure seems to the present authors to be unlikely.

3. The magnetic structure

There has been general agreement from the earliest determinations (Bertaut & Mercier, 1963; Bertaut *et al.*, 1965; Fiebig *et al.*, 2000) that the magnetic ordering at ~ 70 K produces a triangular antiferromagnetic arrangement of moments on the Mn^{3+} ions in the basal planes, but there has been some discussion of the detail of this arrangement. Here we note that any such arrangement would (like the structural transition) cause a tripling of the cell of the $P6_3/mmc$ parent structure, and hence be driven by an irrep at the *K*-point ($\boldsymbol{k}$ = 1/3,1/3,0) of the Brillouin zone. It is found using *ISOTROPY* (Stokes *et al.*, 2007) that the only irreps putting the moments in the basal plane are mK_2, mK_3 and mK_6. Of these the two-dimensional irreps (for magnetic distortions), mK_2 and mK_3 can preserve the crystallographic 6_3 symmetry, whereas the four-dimensional irrep mK_6 cannot. For this reason we will restrict our attention to irreps mK_2 and mK_3. The magnetic structures arising from the action of these two different irreps, and with different values for the order parameters are illustrated in Fig. 2. In this figure it is possible to recognize most of the magnetic structures proposed to date, even though, strictly, they are proposed as arrangements arising after the K_3 structural distortion. The α- and β-models shown by Bertaut & Mercier (1963) appear here as those generated by $mK_3(0,b)$ and $mK_3(a,0)$, respectively. Bertaut & Mercier found that they could fit their neutron data with either of these models but, because the two arrangements lead to identical magnetic structure factors (a circumstance termed homometry), they could not distinguish between them by neutron diffraction. In the end, Bertaut *et al.* (1965) favoured the α-model, corresponding to $mK_3(0,b)$. More generally (Bacon, 1975; Fiebig *et al.*, 2000; Brown & Chatterji, 2006), the α- and β-models are taken to refer to the situations in which corresponding moments in successive layers are parallel and antiparallel, respectively – by this definition the arrangements shown at $mK_2(0,b)$ and $mK_2(a,0)$ are also α- and β-models, respectively. There is also a connection of the patterns shown under $mK_3(a,b)$ with what Goltsev *et al.* (2003) describe as 'solitons'. The α- and β-type arrangements with moments at arbitrary angles to the crystallographic axes, as considered elsewhere (Bacon, 1975; Fiebig *et al.*, 2000; Brown & Chatterji, 2006), do not appear in our Fig. 2 since they require the simultaneous action of irreps mK_2 and mK_3.

The question of 'homometric' structures merits further discussion. Bertaut & Mercier (1963) were the first to point out that the structures shown here under $mK_3(0,b)$ and $mK_3(a,0)$ give rise to the same set of neutron intensities, and therefore cannot be distinguished using (unpolarized) neutron diffraction. This relates to the special positions, 'x = 1/3', occupied by the Mn atoms in the parent structure. The initial account (Bertaut & Mercier, 1963) was brief, but the matter was considered in more detail by Bacon (1975). The calculation he presents is for the α-model, taking the moments to make an angle γ with the crystallographic axes. It is easy to modify the calculation for the situation in which the sign of γ reverses from one layer to the next, corresponding to the structure shown here under $mK_3(a,b)$. The results are now independent of the angle γ, confirming that the structures shown under $mK_3(a,0)$, $mK_3(a,b)$ and $mK_3(0,b)$ are all homometric – similarly for the magnetic structures relating to irrep mK_2. These homometries can be broken only to the extent that the Mn atoms move from the positions they occupy

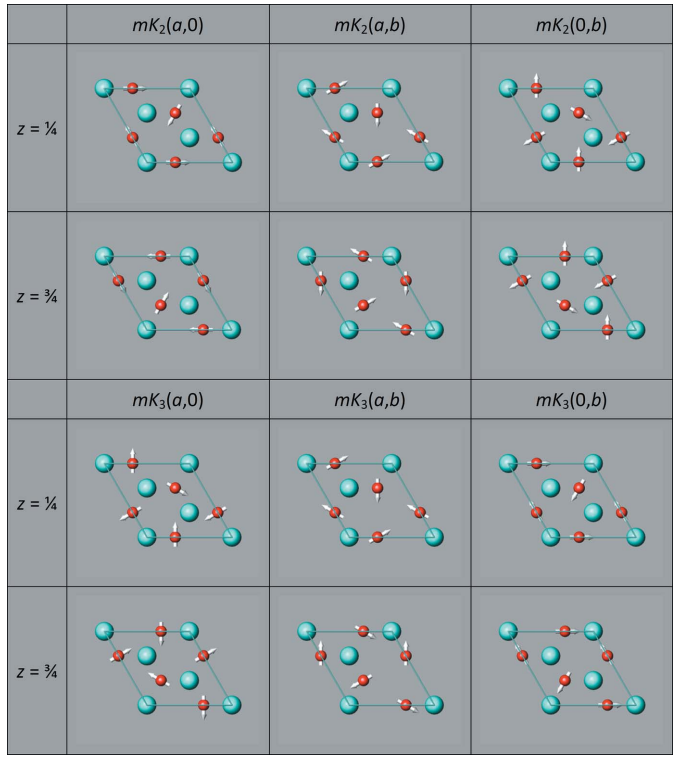

Figure 2
The different magnetic arrangements that can be generated from the $P6_3/mmc$ structure by the action of magnetic distortions mK_2 and mK_3 and different values for the order parameters. The illustrations, generated using *ATOMS*, show the layers at z = 1/4 and z = 3/4, where the Mn ions are to be found. These arrangements are little affected by the addition of the structural distortion.

Table 1
Summary of properties of the different magnetic structures based on space-group symmetry $P6_3cm$.

All these results were obtained using computer programs *ISODISTORT* (Campbell *et al.*, 2006) and *ISOTROPY* (Stokes *et al.*, 2007).

	$P6_3c'm'$	$P6'_3c'm$	$P6_3cm$	$P6'_3cm'$
Derived from $P6_3cm1'$ by	$m\Gamma_2$	$m\Gamma_3$	$m\Gamma_1$	$m\Gamma_4$
Ferroelectric (polarization along z)	√	√	√	√
Admits moments out of xy plane	√	×	×	√
Admits weak ferromagnetism (net along z)	√	×	×	×
Magneto-electric coupling	$P_xM_x + P_yM_y$ P_zM_z	×	$P_xM_y - P_yM_x$	×
Piezo-magnetic coupling	$(e_1 + e_2)M_z$ e_3M_z $e_5M_x + e_4M_y$	$(e_1 - e_2)M_x - e_6M_y$	$e_4M_x - e_5M_y$	$(e_1 - e_2)M_y + e_6M_x$
Second harmonic generation (electric)	$P_zE_zE_z$; $P_zE_xE_x + P_zE_yE_y$; $P_xE_xE_z + P_yE_yE_z$; $P_xE_zE_x + P_yE_zE_y$			
Second harmonic generation (magnetic)	$M_zE_zE_z$ $M_zE_xE_x + M_zE_yE_y$ $M_xE_xE_z + M_yE_yE_z$	$M_xE_yE_y - M_xE_xE_x + 2M_yE_xE_y$	$M_xE_yE_z - M_yE_xE_z$	$M_yE_xE_x - M_yE_yE_y + 2M_xE_xE_y$

Subscripts x, y, z here refer to orthogonal axes, with x and z axes parallel to the crystallographic ***a*** and ***c*** of $P6_3/mmc$, respectively, and the y axis completing the right-handed orthogonal set. The strains, polarizations and magnetizations shown here might need to be substituted by stresses, electric and magnetic fields, respectively, depending on context. The results (invariants) shown here for magneto-electric coupling, piezo-magnetic coupling and SHG (magnetic) are all to be multiplied by the relevant antiferromagnetic order parameter $Q_{\rm AFM}$ to ensure time reversal invariance.

in the parent structures. Brown & Chatterji (2006) attempted to address the problem *via* neutron single-crystal studies using a polarized incident beam. Ideally the diffracted intensities should depend on the direction of polarization, due to interference between nuclear and magnetic scattering. That they did not suggests that the crystal had a domain structure, giving an overall response equivalent, in effect, to what would result from the use of an unpolarized incident beam. Nor was polarimetry (Brown & Chatterji, 2006), based on the measurement of the polarization of the diffracted neutrons, entirely conclusive. The problem of homometry is clearly recognized by some authors (Park *et al.*, 2002; Brown & Chatterji, 2006) but, curiously, not by all (Muñoz *et al.*, 2000).

In Fig. 3, we show different structures arising from the coupling of the structural distortion, driven by $K_3(a,0)$, with

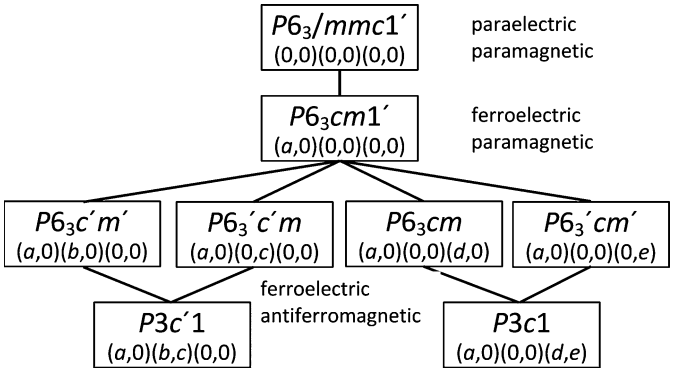

Figure 3
Group–subgroup relationships for the crystal and magnetic structures in $YMnO_3$. The structural transition is taken to be driven by irrep K_3, order parameter $(a,0)$, and the magnetic transition at about 70 K by irreps mK_2 or mK_3 referred to the same paraelectric parent. The diagram indicates the different symmetries possible, each labelled by the values of the order parameters for K_3, mK_2, mK_3, respectively. The lines connect group–subgroup pairs, and where they join such a pair the corresponding transition is allowed to be continuous.

the magnetic ordering which we take to be driven by either mK_2 or mK_3. The figure includes a listing of the order parameters for K_3, mK_2 and mK_3, respectively, for each of the structures obtained. The coupling of the structural distortion with either of the magnetic distortions leads not only to electric polarization, but also to other effects including weak ferromagnetism, some enhancement of the piezomagnetic and magnetoelectric effects, and the potential for second harmonic generation. The properties of the four magnetic structures retaining crystallographic symmetry $P6_3cm$ are summarized in Table 1. Given the difficulty of distinguishing all these structures solely on the basis of neutron diffraction – the homometry discussed above – the final determination of the magnetic structure rests on the examination of various properties as listed here.

As indicated above, Bertaut & Mercier (1963), working from neutron powder diffraction, favoured arrangements derived from irrep mK_3, *i.e.* the (homometric) arrangements with symmetries $P6_3cm$ and $P6'_3cm'$. Bertaut and his coworkers (Bertaut, Pauthenet & Mercier, 1963; Bertaut *et al.*, 1965) claimed to choose between these arrangements on the basis that the former would admit weak ferromagnetism (with none observed); however, according to our analysis (Table 1), neither admits ferromagnetism so that the distinction cannot be made. Neutron powder diffraction was also used in the study by Muñoz *et al.* (2000). These authors too favour the arrangements derived from irrep mK_3 but, curiously, they claim a better fit for the arrangement in $P6_3cm$ than the (homometric) arrangement in $P6'_3cm'$.[2] This claim led to a re-examination of the problem by Park *et al.* (2002). They, like the previous workers, also favoured the arrangements with symmetries $P6_3cm$ and $P6'_3cm'$ but, on the basis of their neutron powder data, could not distinguish between them. Based on their neutron polarimetry from single crystals,

[2] Muñoz *et al.* (2000) employ a notation for irreps differing from the one used here in that Γ_3 and Γ_4 are interchanged.

Brown & Chatterji (2006) favour arrangements near to those derived from irrep mK_3, but claim an 11° rotation of the spins away from the crystallographic axis which would reflect a minor contribution from irrep mK_2.

It can be seen from Table 1 that the observation (or otherwise) of the magneto-electric effect could be used to distinguish the arrangements in a homometric pair. Brown & Chatterji (2006) remark on the 'absence of a magneto-electric effect' in $YMnO_3$ and conclude that the symmetry must include the operation $6'_3$; however, they cite no reference reporting experimental evidence on the claim.[3] Were it not for the 11° rotation, they would have the symmetry as $P6'_3cm'$. Fiebig *et al.* (2000) have used second harmonic generation (SHG) to resolve the ambiguity left by the neutron diffraction. The experimental setup has laser light directed onto a single-crystal platelet along its optic axis, this being the z axis (referenced in Table 1), and the second harmonic is separated from the primary wavelength by use of a prism. The pertinent point is that light is a transverse radiation, so only when there are coupling terms involving just x- and y-components is SHG possible. Starting with the (near) consensus from the neutron studies that the magnetic structure has symmetry $P6_3cm$ or $P6'_3cm'$, along with the observation of SHG by Fiebig *et al.* (2000), leads to the conclusion that the magnetic structure of $YMnO_3$ at low temperature is that with symmetry $P6'_3cm'$. Fiebig *et al.* (2000) confirmed this conclusion by examining the SHG response as the polarization of the incident light was rotated in the xy plane.

It is not clear if the observation of a dielectric anomaly at the Néel point (Huang *et al.*, 1997; Katsufuji *et al.*, 2001) provides any further information on the magnetic symmetry – it seems likely that biquadratic coupling between the structural and magnetic order parameters, which is always allowed, would be sufficient to account for this.

4. Coupling of ferroelectric and magnetic domains

Fiebig *et al.* (2002) have employed sophisticated SHG techniques to image domains in platelets of $YMnO_3$. The ferroelectric domains are of course already extant at room temperature, and different magnetic domains are formed within them. In this context, it is perhaps not surprising that the boundary of a ferroelectric domain should also form the boundary for a magnetic domain. The result that is surprising is that at every ferroelectric domain boundary (*i.e.* where the polarization reverses sign) the magnetic order parameter also reverses sign. To put this another way, the sign of the product of the ferroelectric and magnetic order parameters is conserved across ferroelectric domain boundaries, but apparently not within the ferroelectric domains themselves.

There being no linear magneto-electric coupling in $YMnO_3$, and indeed no net magnetization (assuming symmetry $P6'_3cm'$), this phenomenon has proved difficult to explain. The proposed explanations depend on the premise that the material has lower symmetry at the ferroelectric domain boundary. Fiebig and co-workers (Goltsev *et al.*, 2003; Fiebig *et al.*, 2004; Fiebig, 2006) consider that the effect is due to the interaction of the magnetization developed in a magnetic domain wall that crosses a ferroelectric domain boundary, with the effective field developed from the stresses near a ferroelectric domain boundary, *via* the piezomagnetic effect. A ferroelectric domain boundary (reversal of polarization) on the xz plane (of $P6_3/mmc$) will leave no more symmetry than a mirror plane parallel to yz. In this circumstance symmetry requires only $M_x = 0$, so a magnetic domain wall can be expected to develop a magnetization with components M_y and M_z non-zero. It is also supposed that associated with the ferroelectric domain boundary there will be non-zero stresses σ_{yy}, leading through the piezomagnetic coupling term $[(\sigma_{xx} - \sigma_{yy})H_y + \sigma_{xy}H_x]Q_{AFM}$ to an effective field H_y. The proposition is that the total energy is lowered by interaction of this effective field H_y with the component M_y developed in the magnetic domain wall. In their initial paper Goltsev *et al.* (2003) gave an expression for the variation of M_y across a magnetic domain wall; Wang *et al.* (2010) have extended the analysis by proposing an explicit expression for the variation of σ_{yy} across a ferroelectric domain boundary, and combined this with the result for M_y to derive the interaction energy involved.

An alternative explanation has been offered by Hanamura and co-workers (Hanamura *et al.*, 2003; Hanamura & Tanabe, 2006). The explanation makes reference first to an 'antisymmetric exchange interaction' (Dzyaloshinski–Moriya; Moriya, 1960), but favours 'higher-order anisotropy energy' as the primary contributor to the coupling observed. In either case this would seem to depend on the magneto-electric coupling of a non-zero component of magnetization M_z (not allowed in the bulk, but permitted, as we have remarked, near the domain wall) with the polarization P_z. Whatever the explanation, it seems unlikely that the magnetic domains in $YMnO_3$ could be usefully controlled by the application of an electric field.

5. A giant magneto-elastic coupling?

Recent reports (Lee *et al.*, 2005, 2008) of 'giant magneto-elastic coupling' in $YMnO_3$ have attracted a great deal of interest and merit comment here. First we note that magneto-elastic coupling is not rare, and in our own work we have encountered strains associated with magnetic transitions (paramagnetic to antiferromagnetic) ranging from scarcely measurable for $KMnF_3$ (Carpenter *et al.*, 2012), through about 0.4% for haematite (Oravova *et al.*, 2013), to 1% in MnO (Carpenter *et al.*, 2012). From the published lattice parameter data (Lee *et al.*, 2005) we have estimated the strain associated with the magnetic transition at less than 0.05% (Thomson *et al.*, 2014), and recent independent measurements of the strain (Chatterji *et al.*, 2012) indicate the strains at $\sim 0.03\%$. By comparison with the other systems we consider it a misnomer to describe $YMnO_3$ as exhibiting a 'giant magneto-elastic'

[3] Brown & Chatterji (2006) include a reference to Fiebig *et al.* (2002), in which it is stated that the linear magneto-electric effect is symmetry forbidden – but this is far from an experimental determination, and indeed is based on the assumption by Fiebig *et al.* (2002) that the symmetry is known.

effect. In fact, what is being reported (Lee *et al.*, 2008) are large changes in atomic positions, roughly comparable with those recorded in a ferroelectric material such as $BaTiO_3$. The strain associated with the ferroelectric transition in $BaTiO_3$ is in excess of 1% (see, for example, Darlington *et al.*, 1994); thus, if the atomic shifts in $YMnO_3$ were as large as claimed the elastic response would have to be considered surprisingly small.

The atomic positions for which large changes are reported have been obtained, in the first instance (Lee *et al.*, 2005), *via* the Rietveld (1969) method from high-resolution neutron powder diffraction. All the atomic positions obtained showed significant changes below the Néel temperature: for example, the *x* coordinate for Mn (which is 1/3 in the paraelectric phase) was reported at 0.3330 (17) above the magnetic transition and at 0.3423 (13) at 10 K (Lee *et al.*, 2005). Although the increase is nearly 3%, and much more than the indicated errors, it is a concern that different determinations of this parameter show so much scatter – for example, other neutron powder diffraction studies give 0.3208 (18) (Muñoz *et al.*, 2000) and 0.3177 (9) (Gibbs *et al.*, 2011) at room temperature, while Brown & Chatterji (2006) using a neutron single-crystal method with high real space resolution found 0.3335 (6) at 10 K. More seriously, and as already pointed out by Chatterji *et al.* (2012), the nature of the antiferromagnetic ordering in $YMnO_3$ ($\boldsymbol{k} = 0$) is such that in the ordered state there will be a magnetic contribution to every observed reflection, and unless this is accounted for it will impact on the results. That the authors (Lee *et al.*, 2005) of the neutron study showing large atomic shifts did not remark on this problem suggests that they overlooked it, in which case the large changes in atomic positions are very likely just artefacts of the analysis. The large shifts appear to have been confirmed in a subsequent synchrotron X-ray diffraction study (Lee *et al.*, 2008), but this does not allay our concerns.

6. Summary and conclusions

The published data on the hexagonal manganite $YMnO_3$ have been critically reviewed, with particular attention to the structures and symmetries. We conclude that this manganite, which is paraelectric in $P6_3/mmc$ at elevated temperatures, undergoes a structural transition on cooling through 1250 K to a ferrielectric phase in $P6_3cm$ which is retained through room temperature. At a much lower temperature, 70 K, there is a magnetic transition from paramagnetic to a triangular antiferromagnetic arrangement, most likely with symmetry $P6_3'cm'$.

There have been claims in the literature (Lonkai *et al.*, 2004) that the transition from the high-temperature paraelectric $P6_3/mmc$ to the room-temperature ferrielectric structure in $P6_3cm$ should proceed *via* an intermediate phase, but we find the arguments in support of these claims flawed and the experimental evidence less than compelling. In our view there is a single transition driven by an irrep K_3 at the *K*-point, ($\boldsymbol{k}$ = 1/3,1/3,0).

Different proposed antiferromagnetic ordering patterns have been examined. These can be considered as arising from the combination of *K*-point structural and magnetic distortions of the high-temperature paraelectric $P6_3/mmc$, or from Γ-point ($\boldsymbol{k}$ = 0) magnetic distortions of the ferrielectric structure in $P6_3cm$. These different structures cannot all be distinguished using neutron diffraction; in particular, structures arising from the same *K*-point irrep give essentially identical neutron patterns. The (near) consensus from neutron diffraction experiments is that the magnetic structure is one of those arising from irrep mK_3 (referencing the paraelectric structure), or from $m\Gamma_1$ or $m\Gamma_4$ with respect to the ferrielectric structure. The magnetic symmetries of these structures are $P6_3cm$ and $P6_3'cm'$. The ambiguity left by the neutron studies has been resolved by examining other physical properties and, in particular, the observation of second harmonic generation when light is incident along the hexagonal axis appears to establish the structure as that with symmetry $P6_3'cm'$.

Further second harmonic generation studies (Fiebig *et al.*, 2002) reveal interesting domain behaviour – the magnetic domains are formed in such a way that at every ferroelectric domain boundary (*i.e.* where the polarization reverses sign) the magnetic order parameter also reverses sign. Since in symmetry $P6_3'cm'$ there can be no linear magneto-electric coupling, and indeed no net magnetization, this phenomenon has proved difficult to explain. The explanations depend on the idea that the symmetry will be lower at a ferroelectric domain boundary, with probably just one mirror plane preserved. With the symmetry lowered in this way, the net magnetization need not be zero, and perhaps even magneto-electric coupling is allowed.

We finished with remarks on the so-called 'giant magneto-elastic coupling' (Lee *et al.*, 2008), a subject which has attracted considerable interest. The term is a misnomer, since the report is of significant shifts in atomic positions below the magnetic ordering temperature, the elastic response being in fact surprisingly small. We speculate, along with Chatterji *et al.* (2012), that the reported atomic shifts are an artefact of a Rietveld analysis in which the magnetic intensities have been ignored.

One of the authors (CJH) acknowledges a useful exchange of views with Dr Tapan Chatterji on the matter of the 'giant magneto-elastic coupling', in advance of his recent publication.

References

Abrahams, S. C. (2009). *Acta Cryst.* B**65**, 450–457.
Aken, B. B. van, Meetsma, A. & Palstra, T. T. M. (2001). *Acta Cryst.* C**57**, 230–232.
Bacon, G. E. (1975). *Neutron Diffraction*, 3rd ed, Section 14.5. Oxford: Clarendon Press.
Benedek, N. A., Mulder, A. T. & Fennie, C. J. (2012). *J. Solid State Chem.* **195**, 11–20.
Bertaut, E. F., Fang, P. & Forrat, F. (1963). *C. R. Hebd. Seances Acad. Sci.* **256**, 1958.
Bertaut, E. F. & Mercier, M. (1963). *Phys. Lett.* **5**, 27–29.
Bertaut, E. F., Pauthenet, R. & Mercier, M. (1963). *Phys. Lett.* **7**, 110–111.

Bertaut, E. F., Pauthenet, R. & Mercier, M. (1965). *Phys. Lett.* **18**, 13.
Brown, P. J. & Chatterji, T. (2006). *J. Phys. Condens. Matter*, **18**, 10085–10096.
Campbell, B. J., Stokes, H. T., Tanner, D. E. & Hatch, D. M. (2006). *J. Appl. Cryst.* **39**, 607–614.
Carpenter, M. A., Salje, E. K. H. & Howard, C. J. (2012). *Phys. Rev. B*, **85**, 224430.
Carpenter, M. A., Zhang, Z. & Howard, C. J. (2012). *J. Phys. Condens. Matter*, **24**, 156002.
Chatterji, T., Ouladdiaf, B., Henry, P. F. & Bhattacharya, D. (2012). *J. Phys. Condens. Matter*, **24**, 336003.
Christy, A. G. (1995). *Acta Cryst.* B**51**, 753–757.
Darlington, C. N. W., David, W. I. F. & Knight, K. S. (1994). *Phase Transitions*, **48**, 217–236.
Dowty, E. (1999). *ATOMS*, Version 5.07. Shape Software, Kingsport, Tennessee, USA.
Eerenstein, W., Mathur, N. D. & Scott, J. F. (2006). *Nature*, **442**, 759–765.
Fennie, C. J. & Rabe, K. M. (2005). *Phys. Rev. B*, **72**, 100103.
Fiebig, M. (2005). *J. Phys. D Appl. Phys.* **38**, R123–R152.
Fiebig, M. (2006). *Phase Transitions*, **79**, 947–956.
Fiebig, M., Fröhlich, D., Kohn, K., Leute, St., Lottermoser, Th., Pavlov, V. V. & Pisarev, R. V. (2000). *Phys. Rev. Lett.* **84**, 5620–5623.
Fiebig, M., Goltsev, A. V., Lottermoser, Th. & Pisarev, R. V. (2004). *J. Magn. Magn. Mater* **272**, 353–354.
Fiebig, M., Lottermoser, T., Fröhlich, D., Goltsev, A. V. & Pisarev, R. V. (2002). *Nature*, **419**, 818–820.
Gibbs, A. S., Knight, K. S. & Lightfoot, P. (2011). *Phys. Rev. B*, **83**, 094111.
Goltsev, A. V., Pisarev, R. V., Lottermoser, T. & Fiebig, M. (2003). *Phys. Rev. Lett.* **90**, 177204.
Hanamura, E., Hagita, K. & Tanabe, Y. (2003). *J. Phys. Condens. Matter*, **15**, L103–L109.
Hanamura, E. & Tanabe, Y. (2006). *Phase Transitions*, **79**, 957–971.
Howard, C. J. & Carpenter, M. A. (2012). *Acta Cryst.* B**68**, 209–212.
Howard, C. J. & Stokes, H. T. (2005). *Acta Cryst.* A**61**, 93–111.
Huang, Z. J., Cao, Y., Sun, Y. Y., Xue, Y. & Chu, C. W. (1997). *Phys. Rev. B*, **56**, 2623–2626.
Katsufuji, T., Mori, S., Masaki, M., Moritomo, Y., Yamamoto, N. & Takagi, H. (2001). *Phys. Rev. B*, **64**, 104419.
Kim, J., Koo, Y. M., Sohn, K. & Shin, N. (2010). *Appl. Phys. Lett.* **97**, 092902.
Lee, S., Pirogov, A., Han, J. H., Park, J.-G., Hoshikawa, A. & Kamiyama, T. (2005). *Phys. Rev. B*, **71**, 180413.
Lee, S., Pirogov, A., Kang, M., Jang, K. H., Yonemura, M., Kamiyama, T., Cheong, S. W., Gozzo, F., Shin, N., Kimura, H., Noda, Y. & Park, J. G. (2008). *Nature*, **451**, 805–808.
Lonkai, T., Tomuta, D. G., Amann, U., Ihringer, J., Hendrikx, R. W. A., Többens, D. M. & Mydosh, J. A. (2004). *Phys. Rev. B*, **69**, 134108.
Miller, S. C. & Love, W. F. (1967). *Tables of Irreducible Representations of Space Groups and Co-representations of Magnetic Space Groups.* Boulder: Pruett.
Moriya, T. (1960). *Phys. Rev.* **120**, 91–98.
Muñoz, A., Alonso, J. A., Martínez-Lope, M. J., Casáis, M. T., Martínez, J. L. & Fernández-Díaz, M. T. (2000). *Phys. Rev. B*, **62**, 9498–9510.
Oravova, L., Zhang, Z., Church, N., Harrison, R. J., Howard, C. J. & Carpenter, M. A. (2013). *J. Phys. Condens. Matter*, **25**, 116006.
Park, J., Kong, U., Pirogov, A., Choi, S. I., Park, J.-G., Choi, Y. N., Lee, C. & Jo, W. (2002). *App. Phys. A*, **74**, s796–s798.
Rietveld, H. M. (1969). *J. Appl. Cryst.* **2**, 65–71.
Smolenski, G. A. & Bokov, V. A. (1964). *J. Appl. Phys.* **35**, 915.
Stokes, H. T., Hatch, D. M. & Campbell, B. J. (2007). *ISOTROPY*, http://stokes.byu.edu/isotropy.html.
Thomson, R. I., Chatterji, T., Howard, C. J., Palstra, T. T. M. & Carpenter, M. A. (2014). *J. Phys. Condens. Matter*. Accepted for publication.
Van Aken, B. B., Palstra, T. T. M., Filippetti, A. & Spaldin, N. A. (2004). *Nature Mater.* **3**, 164–170.
Wang, Z., Huang, F. Z., Lu, X. M. & Zhu, J. S. (2010). *Eur. Phys. J. B*, **75**, 217–221.
Yakel, H. L., Koehler, W. C., Bertaut, E. F. & Forrat, E. F. (1963). *Acta Cryst.* **16**, 957–962.